A supramolecular gel based on a glycosylated amino acid derivative with the property of gel to crystal transition

Jie Liu,[a] Fengyang Xu,[a] Ziling Sun,*[b] Yue Pan,[a] Jian Tian,[b] Hsin-Chieh Lin,[c] Xinming Li*[a]

Supporting information

1) NMR and LC-MS of Fmoc-Asp(Glc)-OtBu

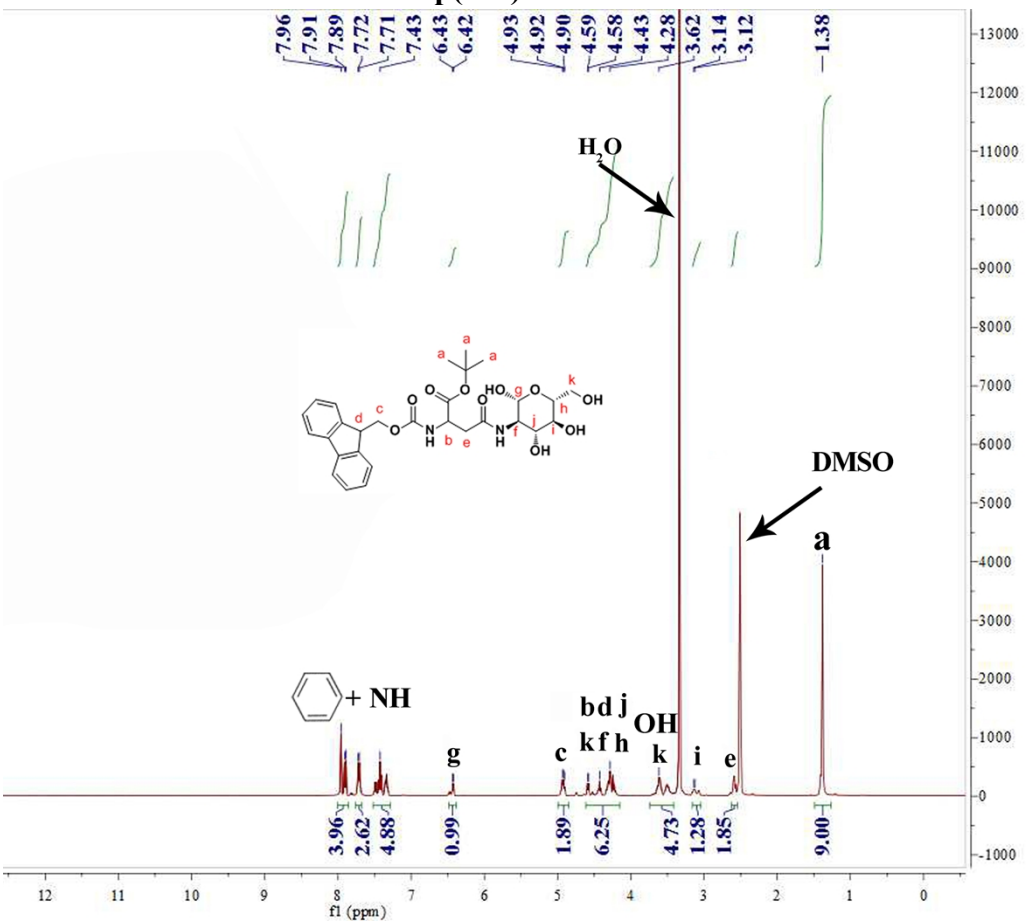

Fig. S1 ^{1}H NMR of Fmoc-Asp(Glc)-OtBu in DMSO-d_6.

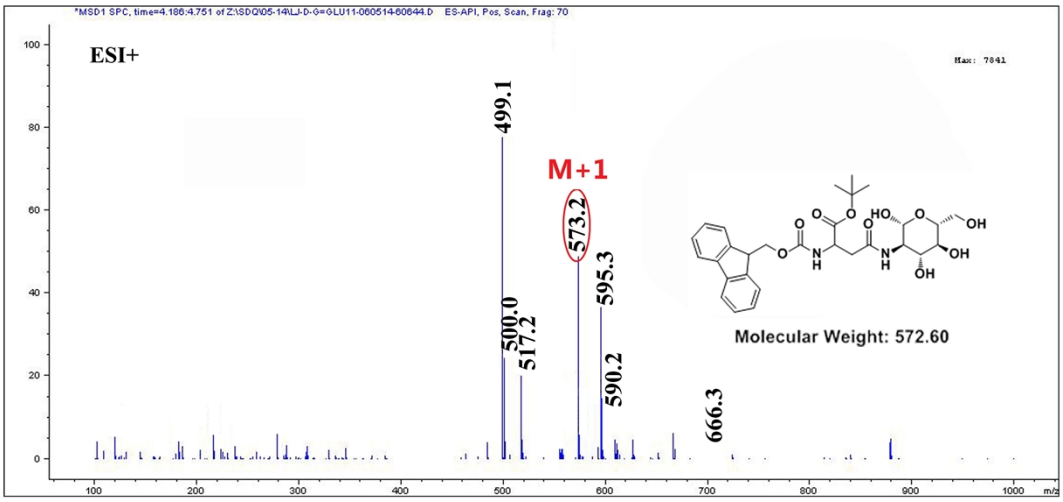

Fig. S2 LC-MS of Fmoc-Asp(Glc)-OtBu.

2) Self-assembling properties of Fmoc-Asp(Glc)-OtBu in the solvents of chlorobenzene, *m*-dichlorobenzene, *o*-dichlorobenzene and xylene, respectively.

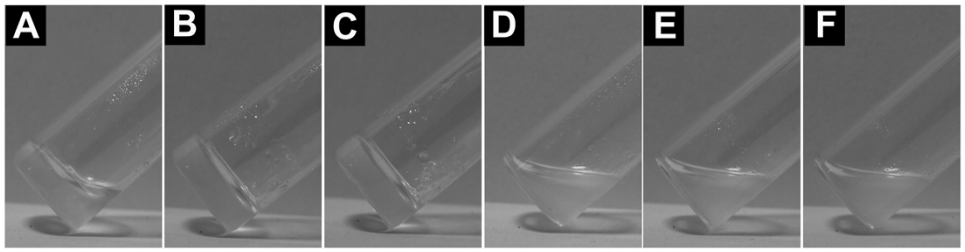

Fig. S3 Optical images of the organogels and solutions in different solvents. (A) chlorobenzene, 4.5 wt%, 25 °C; (B) *o*-dichlorobenzene, 4.5 wt%, 25°C; (C) *m*-dichlorobenzene, 5.0 wt%, 25°C; (D) *o*-xylene, 5.0 wt%, 25°C; (E) *m*-xylene 5.0 wt%, 25 °C; (F) *p*-xylene 5.0 wt%, 25 °C.

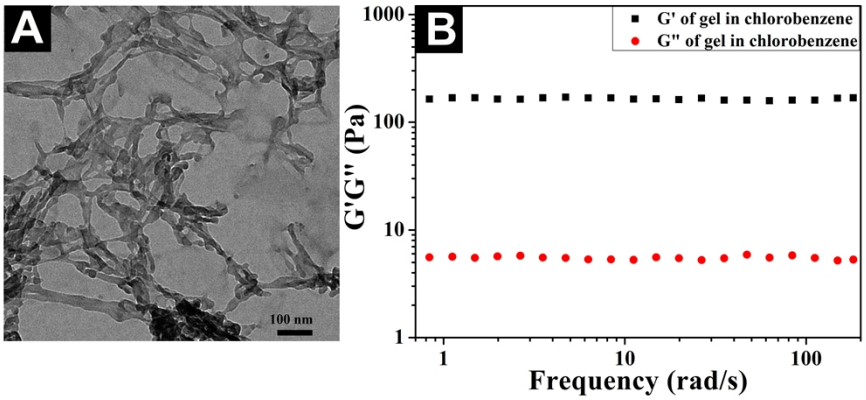

Fig. S4 TEM image (A) and frequency dependence (B) of the dynamic storage moduli (*G'*) and the loss moduli (*G''*) of the organogels formed in chlorobenzene in Fig. S3A.

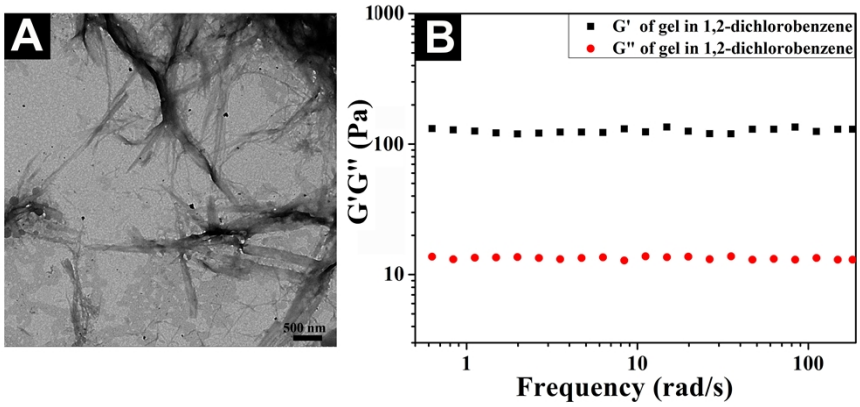

Fig. S5 TEM image (A) and frequency dependence (B) of the dynamic storage moduli (G') and the loss moduli (G'') of the organogels formed in *o*-dichlorobenzene in Fig. S3B.

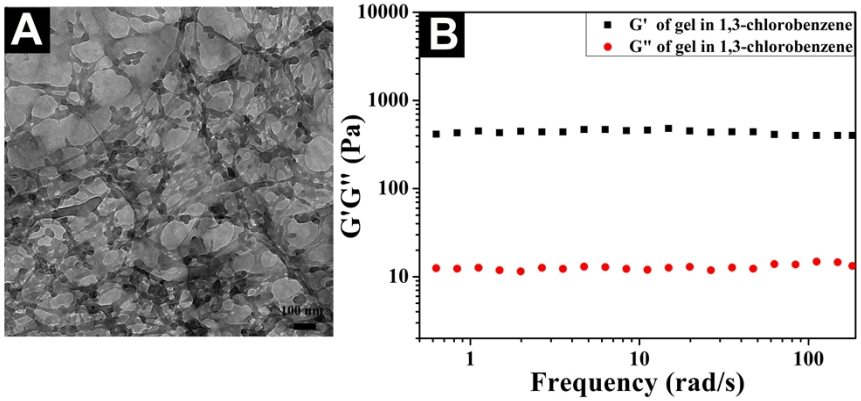

Fig. S6 TEM image (A) and frequency dependence (B) of the dynamic storage moduli (*G'*) and the loss moduli (*G''*) of the organogels formed in *m*-dichlorobenzene in Fig. S3C.

3) Self-assembling properties of Fmoc-Asp(Glc)-OtBu in the mixed solvents of water and ethanol

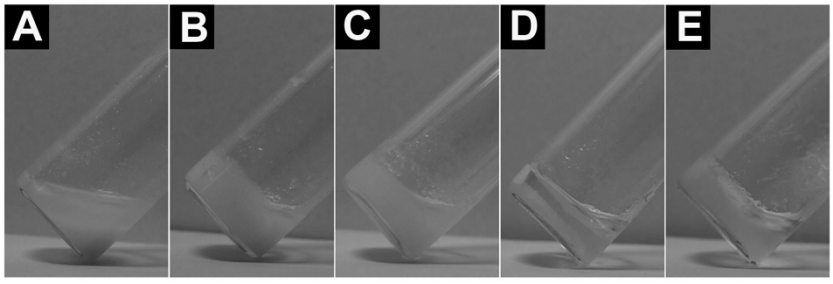

Fig. S7 Optical images of the organogels formed in the mixed solvents of water and ethanol. (A) water, 2.5 wt%, 25 °C; (B) water:ethanol=75:25, 2.5 wt%, 25°C; (C) water:ethanol=60:40, 2.7 wt%, 25°C; (D) water:ethanol=40:60, 3.7 wt%, 25 °C; (E) water:ethanol=25:75, 4.7 wt%, 25 °C.

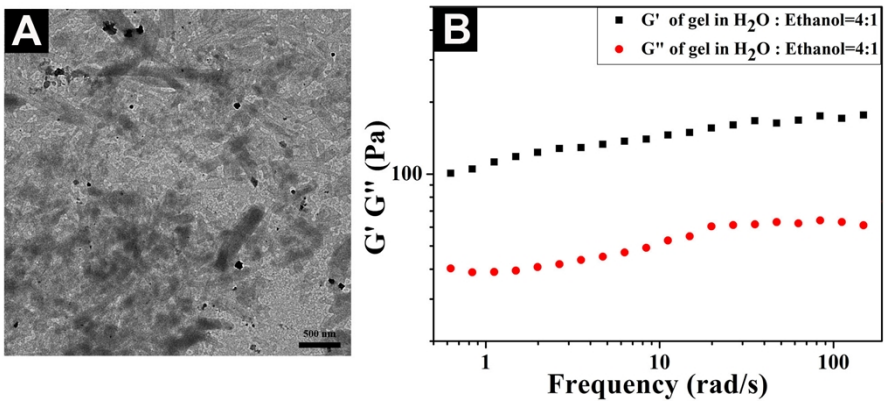

Fig. S8 TEM image (A) and frequency dependence (B) of the dynamic storage moduli (*G'*) and the loss moduli (*G''*) of the organogels formed in the mixed solvent of water and ethanol (75:25) in Fig. S7B.

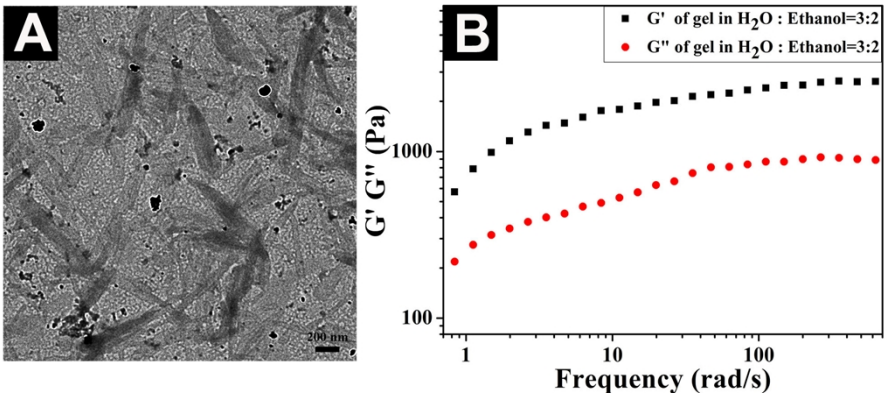

Fig. S9 TEM image (A) and frequency dependence (B) of the dynamic storage moduli (*G'*) and the loss moduli (*G''*) of the organogels formed in the mixed solvent of water and ethanol (60:40) in Fig. S7C.

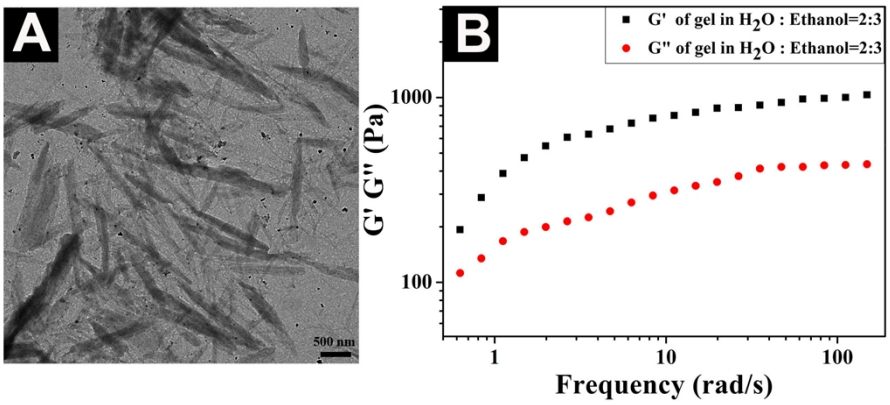

Fig. S10 TEM image (A) and frequency dependence (B) of the dynamic storage moduli (*G'*) and the loss moduli (*G''*) of the organogels formed in the mixed solvent of water and ethanol (40:60) in Fig. S7D.

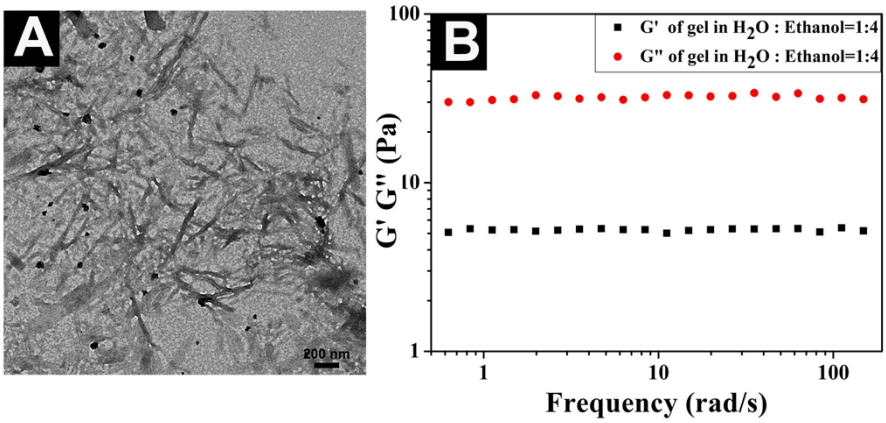

Fig. S11 TEM image (A) and frequency dependence (B) of the dynamic storage moduli (*G'*) and the loss moduli (*G''*) of the organogels formed in the mixed solvent of water and ethanol (25:75) in Fig. S7E.

4) Optical micrographs of microstructure formed by Fmoc-Asp(Glc)-OtBu in different solvents

A small amount of gel or microcrystal sample was carefully picked up and placed on a clean glass slide and observed immediately by an Olympus IX71 optical microscope.

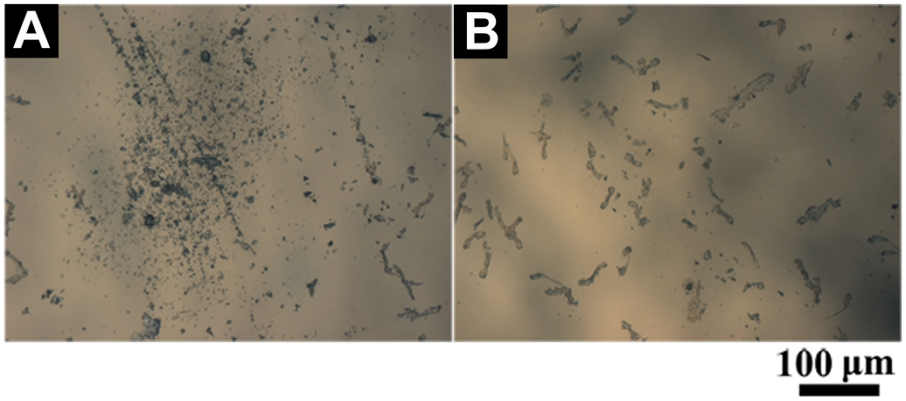

Fig. S12 Optical micrographs of (A) the precipitates appeared at the top of the solution and B) the surrounding solution during the gelation process of Fmoc-Asp(Glc)-OtBu in DCM as shown in Fig. 4.

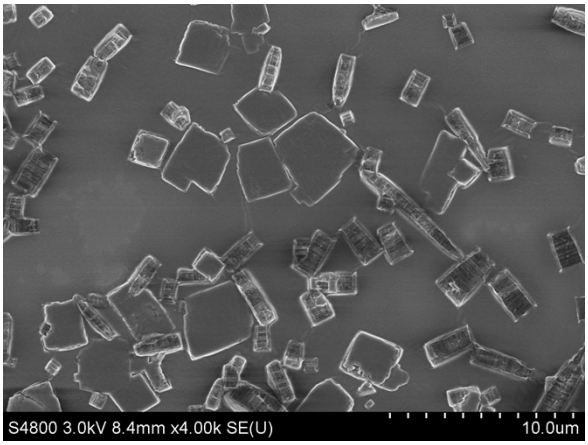

Fig. S13 SEM image of the microcrystals generated in the organogel of DCM after gel to crystal transition shown in Fig.4.

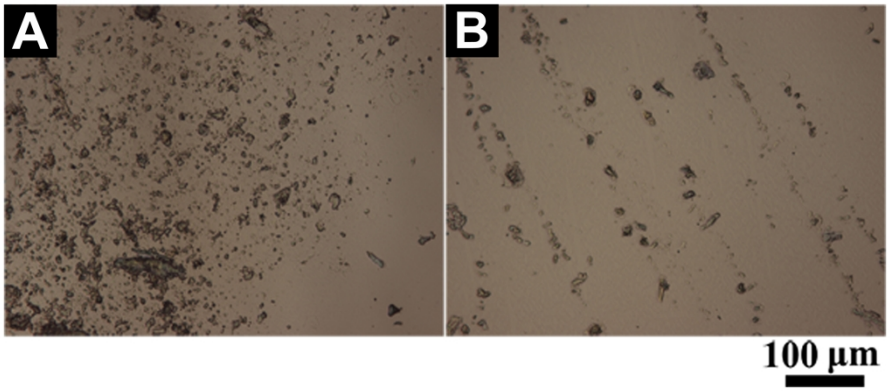

Fig. S14 Optical micrographs of (A) the precipitates appeared at the top of the solution and B) the surrounding solution during the gelation process of Fmoc-Asp(Glc)-OtBu in chloroform shown in Fig. 4.

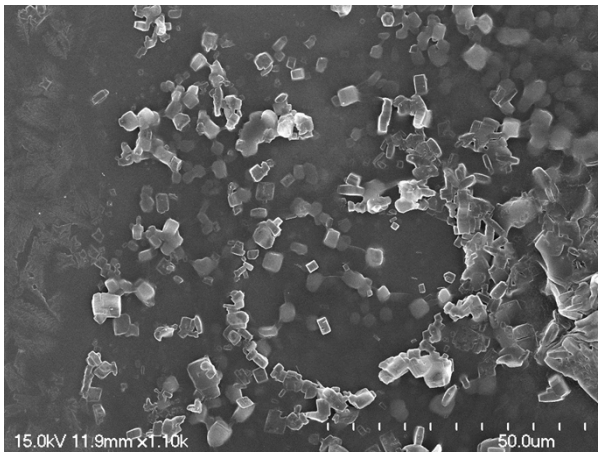

Fig. S15 SEM image of the microcrystals generated in the organogel of chloroform after gel to crystal transition shown in Fig.4.

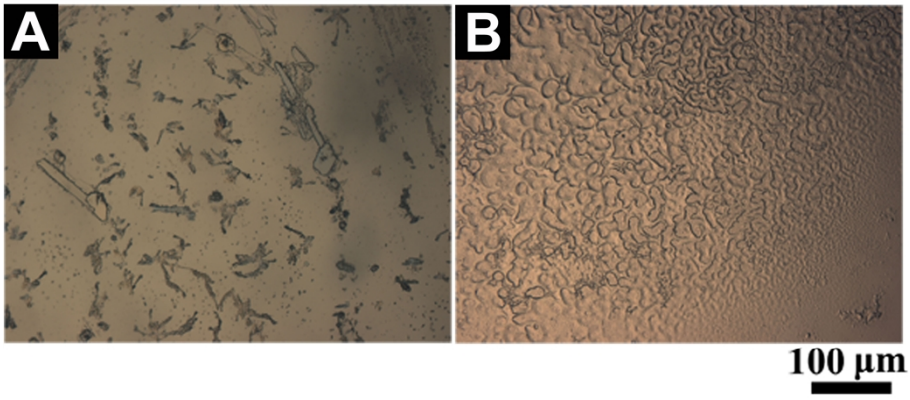

Fig. S16 Optical micrographs of (A) the precipitates appeared at the top of the solution, and B) the surrounding solution during the gelation process of Fmoc-

Asp(Glc)-OtBu in ethanol shown in Fig. 4.

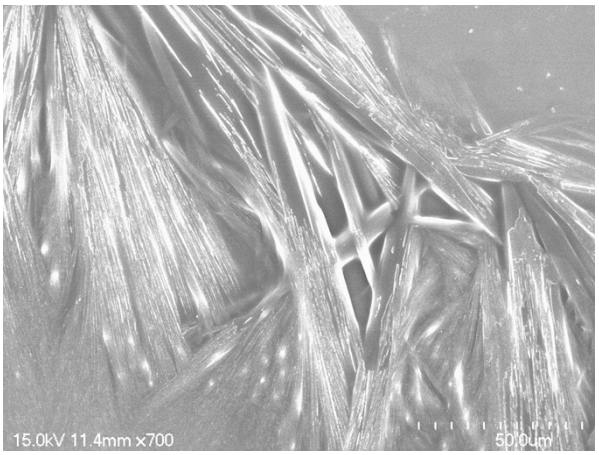

Fig. S17 SEM image of the microcrystals generated in the organogel of ethanol after gel to crystal transition shown in Fig.4.